Phase diagram of two-component bosons on an optical lattice

New Journal of Physics
An Institute of Physics and Deutsche Physikalische Gesellschaft Journal

Phase diagram of two-component bosons on an optical lattice

Ehud Altman, Walter Hofstetter, Eugene Demler and Mikhail D Lukin

Department of Physics, Harvard University, Cambridge, MA 02138, USA
E-mail: altman@fas.harvard.edu

New Journal of Physics **5** (2003) 113.1–113.19 (http://www.njp.org/)
Received 27 June 2003, in final form 14 August 2003
Published 22 September 2003

Abstract. We present a theoretical analysis of the phase diagram of two-component bosons on an optical lattice. A new formalism is developed which treats the effective spin interactions in the Mott and superfluid phases on the same footing. Using this new approach we chart the phase boundaries of the broken spin symmetry states up to the Mott to superfluid transition and beyond. Near the transition point, the magnitude of spin exchange can be very large, which facilitates the experimental realization of spin-ordered states. We find that spin and quantum fluctuations have a dramatic effect on the transition, making it first order in extended regions of the phase diagram. When each species is at integer filling, an additional phase transition may occur, from a spin-ordered insulator to a Mott insulator with no broken symmetries. We determine the phase boundaries in this regime and show that this is essentially a Mott transition in the spin sector.

Contents

PII: S1367-2630(03)65334-6

1. Introduction

Recent observations of the superfluid to Mott insulator transition in a system of ultra-cold atoms in an optical lattice open fascinating prospects for studying many-body phenomena associated with strongly correlated systems in a highly controllable environment [1]–[3]. For instance, theoretical studies have shown that, with spinor bosonic or fermionic atoms in optical lattices, it may be possible to observe complex quantum phase transitions [4], to realize novel superfluidity mechanisms [5] and to probe one-dimensional systems exhibiting spin charge separation [6].

Even the Mott phase of two-component bosons may exhibit rich behaviour. When the motional degrees of freedom are frozen, the remaining pseudospins are coupled by an effective Heisenberg exchange [7]. This effect can be used to 'engineer' interacting spin-$\frac{1}{2}$ Hamiltonians in ultra-cold atoms, opening the door to controlled studies of quantum magnetism [8]. In this approach the two-state bosonic or fermionic atoms are confined in an optical lattice where spin-dependent interactions and hopping are controlled by adjusting the intensity, frequency and polarization of the trapping light.

The effective spin Hamiltonians computed in [7, 8] are valid provided the system is deep in the Mott phase. Then, the motional degrees of freedom are frozen and the effective Heisenberg exchange can be derived by second-order perturbation theory in the tunnelling matrix elements. However, spin effects are expected to be important, and even stronger, at larger values of the tunnelling, where perturbation theory fails. How do the spin interactions affect the transition into a superfluid phase and the properties of the superfluid? This important question cannot be addressed within the perturbative approach that assumes a Mott starting point.

In this paper we present a theoretical framework, which is non-perturbative in the tunnelling and allows us to describe both the superfluid and insulating phases in two-component systems. Using this approach we determine the phase diagram for a total density of one atom per site. We find that the spin-ordered states persist up to the superfluid transition. In this region the critical temperature for spin ordering can be large, facilitating the experimental realization of these phases. The z-antiferromagnetic state (checkerboard occupation of the two components), in particular, enjoys a negative zero-point energy, which extends its domain beyond the mean-field prediction for the Mott phase. The transition between this state and the superfluid is found to be first order in contrast with the standard superfluid–insulator transition.

Before proceeding, we note that spin Hamiltonians can also be simulated by controlled collisions via frequent time-dependent shifts of the lattice potentials [9]. Compared with that method, the spin-dependent tunnelling may have certain experimental advantages since it implements the desired Hamiltonian directly, thus circumventing imperfections and errors associated with rapid perturbations due to the lattice shifts. We also note the recent studies on quantum magnetism induced via magnetic dipole interactions of the condensed atoms [10]. The present approach results in a much larger interaction strength per atom, and also allows for more flexible control over interaction properties.

The paper is organized as follows. In section 2 we describe the Hubbard model for two bosonic species on an optical lattice, which serves as our starting point. In section 3, the perturbative approach of [7, 8] is reviewed and the phase diagram of spin states that arise from it is sketched. We show that, when both species are at integer filling, the phase diagram also includes a Mott transition in the spin sector into an insulator with no broken symmetries. In section 4 we present the mean-field description of the SF–MI (superfluid–Mott insulator) transition in two-component systems. The analytical predictions of a variational approach are compared to

the results of a numerical mean-field analysis. In section 5 a theoretical framework is developed that incorporates the effect of quantum fluctuations and treats the magnetic interactions in the Mott and superfluid phases on an equal footing. Then, in section 6, this framework is used to analyse the full phase diagram at a total filling of one atom per lattice site. The relevance of the present results in the light of realistic experiments is discussed in the concluding paragraphs of this paper.

2. The model

We consider a system with two species of atoms or, equivalently, atoms with two relevant internal states. The two species shall be denoted by the second quantized bosonic operators a and b. We assume that the two species are trapped by independent standing wave laser beams through polarization (or frequency) selection, as done, for example, in [11]. Each laser beam creates a periodic potential in a certain direction $v_{\alpha\sigma}\sin^2(\vec{k}_\alpha\vec{r})$, where $\vec{k}_\alpha$ is the wavevector of the light and $\sigma = a, b$ is the species index. Throughout this work, we assume that the laser beams are orthogonal, creating either a square lattice in two dimensions or a cubic lattice in three dimensions. For sufficiently strong periodic potential and low temperatures the atoms will be confined to the lowest Bloch band. The low-energy Hamiltonian is then given by the Bose–Hubbard model for two boson species:

$$H = -\sum_{\langle ij\rangle} t_a(a_i^\dagger a_j + \text{h.c.}) - t_b\sum_{\langle ij\rangle}(b_i^\dagger b_j + \text{h.c.}) + U\sum_i (n_{ai} - \tfrac{1}{2})(n_{bi} - \tfrac{1}{2}) + \tfrac{1}{2}\sum_{i\alpha=a,b} V_\alpha n_{\alpha i}(n_{\alpha i} - 1) - \sum_{i\alpha}\mu_\alpha n_{\alpha i}. \quad (1)$$

Here $\langle i, j\rangle$ denotes the nearest-neighbour sites and a_i, b_i are bosonic annihilation operators for bosonic atoms of different spin states localized on site i, $n_{ia} = a_{i_\sigma}^\dagger a_{i_\sigma}$, $n_{ib} = b_{i_\sigma}^\dagger b_{i_\sigma}$. For the cubic lattice, using a harmonic approximation around the minima of the potential [3], the spin-dependent tunnelling energies and the on-site interaction energies are given by $t_{a(b)} \approx (\pi^2/4)v_{a(b)}\exp[-(\pi^2/4)(v_{a(b)}/E_\mathrm{R})^{1/2}]$, $U \approx (8/\pi)^{1/2}(ka_{a,b})(E_\mathrm{R}\overline{v}_{ab}^3)^{1/4}$. Here $v_{a,b}$ is the depth of the optical potential for species a and b, $\overline{v}_{ab} = 4v_a v_b/(v_a^{1/2} + v_b^{1/2})^2$ is the spin average potential in each direction, $E_\mathrm{R} = \hbar^2k^2/2m$ is the atomic recoil energy, and a_{ab} is the scattering length between the atoms of different spins. The intra-species interaction is given by $V_{a(b)} \approx (8/\pi)^{1/2}(ka_{a(b)})(E_\mathrm{R}v_{a(b)}^3)^{1/4}$ ($a_{a(b)}$ are the corresponding scattering lengths). Furthermore, the magnitude of the inter-species interaction U can be additionally controlled by shifting the two lattices away from each other, which opens a wide range of U/V_α to exploration. Note that spin-dependent tunnelling $t_{\mu\sigma}$ can be easily introduced by varying the potential depth v_a and v_b with control of the intensity of the trapping laser. We should also point out that the two atomic states generally have different energies ($\mu_a \neq \mu_b$ in (1)). In the spin language, this translates to a magnetic field in the z direction. However, since there is essentially no transfer between the two populations, the experiment is performed with fixed magnetization (population difference $n_a - n_b$) and the chemical potentials can be set to fix this magnetization.

In this paper, we address primarily the case in which the total filling is commensurate with the lattice and the two species have equal density (i.e. zero magnetization). A transition from a superfluid to a Mott insulator is expected, as in the usual case of a single species. However, in this system, magnetic order associated with the pseudospin degrees of freedom (boson components) may occur as well.

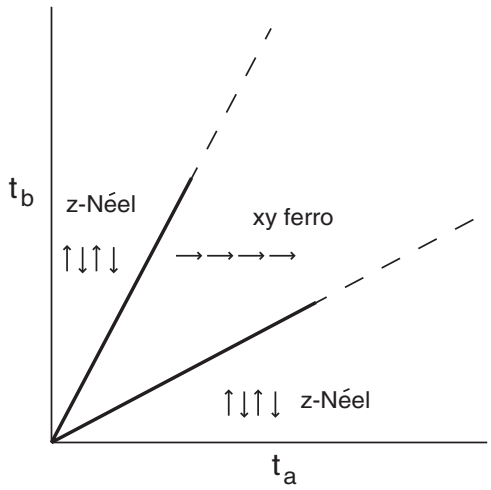

Figure 1. Schematic phase diagram of the effective spin Hamiltonian (2), valid deep in the Mott phase.

3. Deep Mott phase: effective spin Hamiltonian

To illustrate the magnetic orders that can arise it is instructive to begin deep in the Mott insulator in the limit $t_{a,b} \ll U, V_{a,b}$, where the Hamiltonian (1) can be simplified considerably. The low energy Hilbert space in this case contains states with a particular integer occupation on every site. However, there is a remaining degeneracy associated with the spin (boson component) degrees of freedom. The degeneracy can be removed by an effective Hamiltonian acting within the low energy subspace [7, 8]. Consider first the case of total filling of one particle per site where the effective Hamiltonian is easily seen to be

$$H_{\text{eff}} = J_z \sum_{\langle ij \rangle} S_i^z S_j^z - J_\perp \sum_{\langle ij \rangle} (S_i^x S_j^x + S_i^y S_j^y) - h \sum_i S_i^z. \tag{2}$$

Here $|\uparrow\rangle$ and $|\downarrow\rangle$ represent sites occupied by the a and b atoms, respectively, and the couplings, derived by second-order perturbation theory in the tunnelling, are given by

$$\begin{aligned} J_z &= 2\frac{t_b^2 + t_a^2}{U} - \frac{4t_a^2}{V_a} - \frac{4t_b^2}{V_b} \\ J_\perp &= \frac{4t_a t_b}{U} \\ h &= \frac{2t_a^2}{V_a} - \frac{2t_b^2}{V_b} + h_{\text{ext}}. \end{aligned} \tag{3}$$

We assume that the induced ordering field h can be cancelled by an externally applied field h_{ext}. In this case the model obviously exhibits a transition between a x–y ferromagnet for $J_\perp > J_z > 0$ and an Ising antiferromagnet with z-Néel order (figure 1).

We now extend the discussion to the case of any integer filling of N atoms per site. To see how things may become qualitatively different from the singly occupied case, consider first a Mott state with two atoms per site. The low-energy Hilbert space of a lattice site consists of the three states

$$\frac{1}{\sqrt{2}}(a^\dagger)^2|0\rangle, \qquad a^\dagger b^\dagger|0\rangle, \qquad \frac{1}{\sqrt{2}}(b^\dagger)^2|0\rangle. \tag{4}$$

If $V_{a,b} \gg U$, the state $a^\dagger b^\dagger|0\rangle$ has a much lower energy than the other two. This implies a simple Mott state $\prod_i a_i^\dagger b_i^\dagger|0\rangle$ which, unlike the Mott states in figure 1, does not break any symmetries. On the other hand, when $V_{a,b}$ is of the same order as U, all three states should be taken into account and more phases may be possible. Therefore in the general case of N atoms per site we consider the regime $t_{a,b}, |V_{a,b} - U| \ll U$, $V_{a,b}$ and $V_a = V_b$.

The low-energy Hilbert space of a lattice site with N atoms per site can be constructed in a similar way. It contains the $N + 1$ states:

$$|S, m\rangle = \frac{(a^\dagger)^{S+m}}{\sqrt{(S+m)!}} \frac{(b^\dagger)^{S-m}}{\sqrt{(S-m)!}}|0\rangle \tag{5}$$

where $S \equiv N/2$ and $m = -S, \ldots, S$. Obviously $a^\dagger$ and $b^\dagger$ act as Schwinger bosons, creating a multiplet of pseudospin S. The spin magnitude depends on the site occupancy. It is integer for even N and half-integer for odd N.

Now the effective Hamiltonian within the spin S subspace can be derived by second-order perturbation theory [7] as a straightforward generalization of (2). The result is

$$H_{\text{eff}} = -\sum_{\langle ij\rangle}[J_\perp(S_i^x S_j^x + S_i^y S_j^y) + J_z S_i^z S_j^z] + u\sum_i (S_i^z)^2 - h\sum_i S_i^z \tag{6}$$

where the interactions are given by

$$\begin{aligned} u &= V_a - U = V_b - U \\ J_\perp &= \frac{4t_a t_b}{U} \\ J_z &= 2\frac{t_a^2 + t_b^2}{U} \\ h &= z(2S+1)\frac{t_a^2 - t_b^2}{U} + h_{\text{ext}}. \end{aligned} \tag{7}$$

Note that, if we take $S \to \frac{1}{2}$, the parameters are identical to those of the effective spin-$\frac{1}{2}$ Hamiltonian (2) in the case $U \approx V_a = V_b$. Note also that additional terms, such as $(S_i^z S_j^z)^2$, do not arise. The $(S^z)^2$ term is, of course, just a constant for $S = \frac{1}{2}$ and therefore has no effect in this case. However, it plays an important role at larger values of the spin, namely for occupations $N > 1$.

For simplicity, consider first the system in the absence of an ordering field ($h = 0$) or at fixed zero magnetization. When u is small compared to J_z or $J_\perp$, the remaining terms in (6) form an anisotropic Heisenberg model. A standard, coherent state mean-field theory is then possible, which yields x–y ferromagnetic order. A positive u acts to reduce the S_z component of the spins. At large enough u, the classical coherent states that represent fully polarized spins become unsuitable descriptions of the system. Specifically, at large u all spins will be essentially confined to their lowest possible S^z states.

When the spin is half-integer (odd filling), there are two active states, at large u (and $h = 0$), corresponding to $S^z = \pm\frac{1}{2}$. The Hamiltonian (6) then reduces to a spin-$\frac{1}{2}$ model, but the spin interactions remain practically identical. Thus, the essential physics is unchanged and we expect spin-ordered phases as in the singly occupied case.

The behaviour of integer spins (even filling) at $h = 0$ is qualitatively different. At large enough u only the $S^z = 0$ state will be important. We then expect that the system is well described by $|\Psi\rangle = \prod_i |S, m = 0\rangle_i$, a Mott state with no broken symmetries. We should point out that, for $h \neq 0$, we may also obtain such a Mott state for odd total filling (half-integer spin) when the average occupation of each species is integer. The transition from this state, where the relative occupation $n_a - n_b$ is fixed on each site, to the x–y ferromagnet, where the relative occupation is fluctuating, is formally equivalent to a Mott transition. It can be regarded as a Mott transition in the spin sector from a 'spin' insulator to a 'spin', or counterflow, superfluid [7]. The Mott transition from the x–y ferromagnet to the superfluid phase, where also $n_a + n_b$ is fluctuating, occurs in the 'charge' sector.

To describe the 'spin–Mott' transition we note that only the three states with lowest S^z play an important role in its vicinity. We therefore write a homogeneous mean-field ansatz for integer spins:

$$|\Psi\rangle = \prod_i [\cos(\theta/2)|S, 0\rangle + \mathrm{e}^{\mathrm{i}\eta} \sin(\theta/2)(\mathrm{e}^{\mathrm{i}\varphi} \cos(\chi/2)|S, 1\rangle + \mathrm{e}^{-\mathrm{i}\varphi} \sin(\chi/2)|S, -1\rangle)]. \tag{8}$$

For half-integer spins with an ordering field $h \neq 0$ we could write an identical ansatz including only the three states with lowest on-site energy. The variational energy in the state (8) is given by

$$E = -\frac{J_\perp z}{8} S(S+1) \sin^2\theta (1 + \sin\chi \cos 2\eta) - \frac{J_z z}{2} \sin^4\frac{\theta}{2} \cos^2\chi + u \sin^2\frac{\theta}{2} - h \sin^2\frac{\theta}{2} \cos\chi \tag{9}$$

and we see that the minimum occurs for $\eta = 0, \pi$. The x–y order parameter is $\langle S^+ \rangle \propto \sin\theta \equiv \psi$. Therefore, to find the transition to a Mott insulator we expand the energy up to quadratic order in ψ and minimize it with respect to χ. Note that the quartic term is always positive since $J_z < J_\perp$. We then obtain the critical value of $J_\perp$ as a function of h:

$$\frac{J_{\perp c}}{u} = \frac{1 - (h/u)^2}{zS(S+1)}. \tag{10}$$

For magnetic fields $h > u$, the description in terms of the states $\{|-1\rangle, |0\rangle, |1\rangle\}$ breaks down. Instead, a similar scheme can be carried out, using the states $\{|0\rangle, |1\rangle, |2\rangle\}$. This yields another lobe corresponding to a phase with well defined $S^z = 1$. A schematic phase diagram is plotted in figure 2. As the ordering field is increased, we obtain lobes corresponding to larger values of S^z up to $S^z = S$, where the spin is fully polarized. In practice the number of particles in each spin state is conserved independently. In other words the experiment is done with fixed z magnetization and h is used as a theoretical tool to set this magnetization in our model. In what follows we fix zero magnetization by setting $h = 0$.

In summary, we sketched the insulating region of the phase diagram of two-component bosons. When the filling of each species is integer there is a transition from a x–y ferromagnetic state to a Mott state without broken symmetries as the intra-species interaction is increased relative to the inter-species interaction (figure 2). Related spin-ordering transitions for spin-1 bosons have been discussed recently by Imembakov *et al* [13] and Snoek and Zhou [14]. On the other hand, at half-integer filling of each species, the system is well described by a spin-$\frac{1}{2}$ Hamiltonian of the form (2) and only spin-ordered phases arise (figure 1).

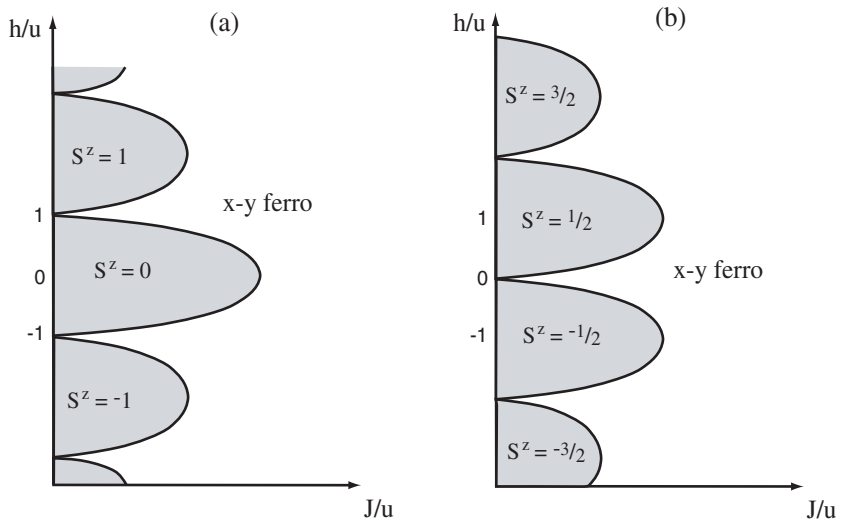

Figure 2. Phase diagram of the Mott state with $0 < V_{a,b} - U \ll U$ and (a) even and (b) odd total filling. The filled lobes mark Mott states with fixed $S^z = (n_a - n_b)/2$. Outside of these lobes the system is also in a Mott state but with x–y ferromagnetic spin order.

The perturbative expansion leading to the effective spin Hamiltonians (2) and (6) breaks down as the transition to a superfluid is approached and $t_{a,b}$ become comparable to U. The question arises as to whether the phases predicted by the effective spin Hamiltonian still hold in this regime. More importantly, how do the effective spin interactions affect the nature of the transition to a superfluid, and the superfluid phase itself?

To answer these questions we shall develop, in the next two sections, a theory which captures the effective spin interactions while still able to describe the transition to a superfluid phase.

4. Mean-field theory of the superfluid–Mott transition

The usual, single-component, Mott transition of bosons is well described by mean-field theory [12, 15]. It is thus natural to start our treatment of the two-component case with a mean-field approach. In order to capture the superfluid phase we extend the regime considered in the previous section to allow for arbitrary ratios of $t_{a,b}/U$. However, we shall confine ourselves to the case of a single atom per site and to the limit $U, t_{a,b} \ll V_a, V_b$. Later we shall consider corrections due to finite intra-species interactions.

In this limit, it is particularly advantageous to use a variational approach, which is equivalent to mean-field theory [16]. The idea is to assume a site factorizable wavefunction associated with hard core bosons, which in our case takes the form

$$|\Phi\rangle = \prod_i \left[\sin\frac{\theta_i}{2}\left(\sin\frac{\chi_i}{2}a_i^\dagger + \cos\frac{\chi_i}{2}b_i^\dagger\right) + \cos\frac{\theta_i}{2}\left(\sin\frac{\eta_i}{2} + \cos\frac{\eta_i}{2}a_i^\dagger b_i^\dagger\right)\right]|0\rangle. \tag{11}$$

This is the most general site-factorizable wavefunction with real coefficients which satisfies the same-species hard core constraint. It is easily verified that allowing complex weights would not improve the variational energy. The enormous reduction in Hilbert space, made possible by

neglecting double occupation, is what makes these states convenient to work with. Specifically, it is easy to calculate expectation values. In addition, we shall see that they facilitate a fluctuation expansion about the mean-field theory. Generalization to include higher occupations is possible but would make the subsequent calculations much more complicated.

In the Mott state, where each site is occupied by exactly one atom, the variational state simplifies even more:

$$|\Phi_{MI}\rangle = \prod_i \left(\mathrm{e}^{\mathrm{i}\varphi/2} \sin\frac{\chi_i}{2} a_i^\dagger + \mathrm{e}^{-\mathrm{i}\varphi/2} \cos\frac{\chi_i}{2} b_i^\dagger \right) |0\rangle. \tag{12}$$

We have added the relative phase to evoke a spin-$\frac{1}{2}$ analogy. Indeed (12) can be viewed as a pseudospin-$\frac{1}{2}$ configuration with $a^\dagger|0\rangle = |\uparrow\rangle$ and $b^\dagger|0\rangle = |\downarrow\rangle$.

The onset of superfluidity is characterized by the development of an order parameter $\sin\theta \neq 0$. More precisely, the superfluid order parameters of the two species in the state $|\Phi\rangle$ are given by

$$\begin{aligned} \langle a\rangle &= \frac{1}{2}\sin\theta\cos\left(\frac{\chi-\eta}{2}\right) \\ \langle b\rangle &= \frac{1}{2}\sin\theta\sin\left(\frac{\chi+\eta}{2}\right). \end{aligned} \tag{13}$$

Now a classical energy functional is defined by the expectation value of (1) in $|\Phi\rangle$. Allowing for two sub-lattice orders in a hypercubic lattice with coordination number z, the energy function is

$$\begin{aligned} E = &-\frac{zt_a}{4}\sin\theta_A\sin\theta_B\cos\left(\frac{\chi_A-\eta_A}{2}\right)\cos\left(\frac{\chi_B-\eta_B}{2}\right) \\ &-\frac{zt_b}{4}\sin\theta_A\sin\theta_B\sin\left(\frac{\chi_A+\eta_A}{2}\right)\sin\left(\frac{\chi_B+\eta_B}{2}\right) + \frac{U}{8}(\cos\theta_A+\cos\theta_B), \end{aligned} \tag{14}$$

where all the variational parameters are assumed to be uniform throughout sub-lattice A (B) and are therefore marked only by a sub-lattice rather than a site index. In the superfluid phase this energy is minimized when both $\cos((\chi_i-\eta_i)/2) = 1$ and $\sin((\chi_i+\eta_i)/2) = 1$, which implies $\chi_i = \eta_i = \pi/2$. The remaining degree of freedom θ is uniform on the lattice and is found by minimizing

$$E(\theta) = -\frac{z}{4}(t_a+t_b)\sin^2(\theta) + \frac{U}{4}\cos\theta. \tag{15}$$

The result is

$$\theta = \begin{cases} \pi & t_a+t_b < t_c \\ \mathrm{acos}(-t_c/(t_a+t_b)) & t_a+t_b > t_c \end{cases} \tag{16}$$

where $t_c = U/2z$. We thus find a transition to a Mott insulating state for $t_a + t_b < t_c$, as illustrated by the circles in figure 3. This constitutes a straightforward generalization of the standard transition for a single species.

By assuming the variational state (11), we neglected contributions from states with multiply occupied a or b bosons. To determine effects arising from the finite magnitude of the intra-species interaction we use a numerical self-consistent mean-field theory of (1). As first proposed in [15], the kinetic energy terms in the Hamiltonian are decoupled:

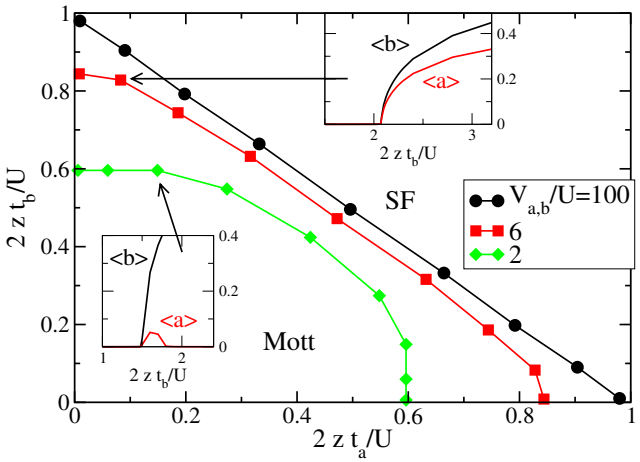

Figure 3. Phase diagram obtained by the decoupling mean-field theory (17) for $U = 20$ and different values of $V_{a,b}$. Note that for finite $V_{a,b}$ and strong asymmetry of the hopping $t_{a,b}$ one of the species can be completely depopulated in the superfluid phase (see the lower left inset). Except for this case, the Mott transition always happens at the same parameters for both species.

$$H_{MF} = U\sum_i (n_{ai} - \tfrac{1}{2})(n_{bi} - \tfrac{1}{2}) + \tfrac{1}{2}\sum_{i;\alpha=a,b} V_\alpha n_{\alpha i}(n_{\alpha i} - 1)$$
$$- \sum_{\langle ij\rangle} t_\alpha (a_i^\dagger \langle a_j\rangle + \text{h.c.}) - t_b \sum_{\langle ij\rangle} (b_i^\dagger \langle b_j\rangle + \text{h.c.}) + \text{constant}. \tag{17}$$

In the homogeneous phase this leads to a sum of identical single-site Hamiltonians:

$$\tilde{H}_{MF} = U(n_a - \tfrac{1}{2})(n_b - \tfrac{1}{2}) + \tfrac{1}{2}\sum_{\alpha=a,b} V_\alpha n_\alpha (n_\alpha - 1) - \Psi_a(a^\dagger + \text{h.c.}) - \Psi_b(b^\dagger + \text{h.c.}) \tag{18}$$

where the *decoupling fields* have to be determined self-consistently according to

$$\Psi_{a,b} = z t_{a,b} \langle a(b)\rangle. \tag{19}$$

We have solved the combined set of equations (18) and (19) numerically by diagonalizing $\tilde{H}_{MF}$ within a finite-size Hilbert space where we allow for up to $M = 9$ bosons per species.

We show results in figure 3, where it can be seen that, for a small ratio $U/V_{a,b}$, the phase diagram is identical to that determined variationally. As $V_{a,b}$ decreases and approaches U the Mott domain shrinks. For $V_{a,b} < U$ there is an instability toward a z-ferromagnetic superfluid. Since the experiment is done at fixed magnetization this would lead to phase separation into domains occupied only by a or b atoms.

Note that in the Mott state where the order parameters $\langle a\rangle$ and $\langle b\rangle$ vanish, the ground state of H_{MF} has precisely one atom per site but is completely independent of the relative weights of a and b atoms. Similarly, the variational energy in the Mott state (12) is a constant ($-U/4$), independent of the individual spin orientation. Thus the simple mean-field approaches are unable to resolve spin order in the Mott state. To obtain spin order we shall in the next section consider quantum fluctuations around the variational mean-field solutions.

5. Effect of fluctuations: 'magnetic' states

The situation we encountered when attempting to treat the Mott phase with the variational states is similar to the basic problem of frustrated quantum magnets. The classical energy of such systems, i.e. the expectation value of the Hamiltonian in a basis of coherent spin states, often contains a macroscopic degeneracy (see, for example, the review [17]). A general mechanism that can lift the degeneracy is 'quantum order by disorder', whereby broken symmetry configurations are selected by the zero-point energy due to spin waves [18].

A spin wave expansion in magnetism includes the quadratic fluctuations around coherent-state mean-field configurations. We formulate a similar expansion in fluctuations about the mean-field states (11). As a first step we define second quantized bosonic operators that create the appropriate Hilbert space:

$$\{a_i^\dagger|0\rangle, b_i^\dagger|0\rangle, a_i^\dagger b_i^\dagger|0\rangle, |0\rangle\} \equiv \{\alpha_{1i}^\dagger|\Omega\rangle, \alpha_{2i}^\dagger|\Omega\rangle, p_i^\dagger|\Omega\rangle, h_i^\dagger|\Omega\rangle\}, \tag{20}$$

where $|\Omega\rangle$ is the vacuum of the new bosons and $|0\rangle$ is an empty site. The new operators are analogues of Schwinger bosons in spin systems and they obey a similar constraint:

$$\alpha_{1i}^\dagger\alpha_{1i} + \alpha_{2i}^\dagger\alpha_{2i} + p_i^\dagger p_i + h_i^\dagger h_i = 1. \tag{21}$$

Now, we apply an orthogonal change of basis:

$$\begin{pmatrix} \psi_{0i} \\ \psi_{1i} \\ \psi_{2i} \\ \psi_{3i} \end{pmatrix} = \begin{pmatrix} \sin\frac{\theta_i}{2}\sin\frac{\chi_i}{2} & \sin\frac{\theta_i}{2}\cos\frac{\chi_i}{2} & \cos\frac{\theta_i}{2}\sin\frac{\eta_i}{2} & \cos\frac{\theta_i}{2}\cos\frac{\eta_i}{2} \\ \cos\frac{\theta_i}{2}\sin\frac{\chi_i}{2} & \cos\frac{\theta_i}{2}\cos\frac{\chi_i}{2} & -\sin\frac{\theta_i}{2}\sin\frac{\eta_i}{2} & -\sin\frac{\theta_i}{2}\cos\frac{\eta_i}{2} \\ \cos\frac{\chi_i}{2} & -\sin\frac{\chi_i}{2} & 0 & 0 \\ 0 & 0 & \cos\frac{\eta_i}{2} & -\sin\frac{\eta_i}{2} \end{pmatrix} \begin{pmatrix} \alpha_{1i} \\ \alpha_{2i} \\ p_i \\ h_i \end{pmatrix}. \tag{22}$$

Note the first row of this rotation. It is chosen in such a way that the variational state (11) would be a simple, singly occupied Fock state of the ψ_0 boson:

$$|\Phi\rangle = \prod_i \psi_{0i}^\dagger|\Omega\rangle. \tag{23}$$

The remaining rows of (22) define a convenient orthonormal basis for the subspace orthogonal to $\psi_0^\dagger|\Omega\rangle$. Thus, the bosons $\psi_{1,2,3}^\dagger$, create fluctuations about the variational state. Of course any other choice of orthonormal basis for the fluctuation subspace would do just as well.

The Hamiltonian (1) acting within the constrained Hilbert space, which excludes multiple occupation by the same species, may be written in terms of the ψ bosons. Furthermore, ψ_{0i} can be eliminated using the hard core constraint

$$\psi_{\beta i}^\dagger\psi_{0i} = \psi_{\beta i}^\dagger\sqrt{1 - \sum_{\alpha=1}^{3}\psi_{\alpha i}^\dagger\psi_{\alpha i}}. \tag{24}$$

Thus the Hamiltonian is a function of only the three fluctuation operators $\psi_{1,2,3}$. Assuming the fluctuations are small, in the sense that their density in the ground state is low, we expand the Hamiltonian to quadratic order in these operators. The exact form of the resulting quadratic Hamiltonian depends on the variational starting point which fixes the rotation matrix (22). For a two sub-lattice variational state, the fluctuation Hamiltonian has the general form:

$$H_{\text{fluc}} = E_{\text{var}} + \tfrac{1}{2}\sum_{\boldsymbol{k}}\left\{\boldsymbol{\Psi}_k^\dagger\begin{pmatrix}\mathcal{F}_k & \mathcal{G}_k \\ \mathcal{G}_k^\star & \mathcal{F}_k^\star\end{pmatrix}\boldsymbol{\Psi}_k - \operatorname{tr}\mathcal{F}_k\right\} \tag{25}$$

where

$$\Psi_k^\dagger = (\psi_k^\dagger \quad \psi_{k+\pi}^\dagger \quad \psi_{-k}^{\mathcal{T}} \quad \psi_{-k+\pi}^{\mathcal{T}}), \qquad \psi_k^\dagger = (\psi_{1k}^\dagger \quad \psi_{2k}^\dagger \quad \psi_{3k}^\dagger) \tag{26}$$

while $\mathcal{F}_k$ and $\mathcal{G}_k$ are 6×6 matrices which depend on the variational parameters. Finally $H_{\rm fluc}$ is diagonalized by a Bogoliubov transformation to obtain the excitation frequencies $\omega_{\alpha k}$ and the correction to the ground state energy:

$$\Delta E = \tfrac{1}{2} \sum_k \left\{ -\mathrm{tr}\, \mathcal{F}_k + \sum_\alpha \omega_{\alpha k} \right\}. \tag{27}$$

With the Bogoliubov transformation at hand it should be straightforward to calculate the average occupation of the fluctuations. For consistency of our approach we require

$$\sum_{\alpha=1}^{3} \langle \psi_{\alpha i}^\dagger \psi_{\alpha i} \rangle \ll 1. \tag{28}$$

Let us now focus on the Mott phase. Recall that the variational energy is independent of the individual spin orientations, i.e. of the parameters in the state (12). The fluctuation Hamiltonian, on the other hand, *will* depend on the spin configuration. Before we compare the zero-point energies corresponding to possible spin orders let us note a few general properties of the fluctuations in this case. Since the bosons $p_i^\dagger$ and $h_i^\dagger$, which create an extra particle or hole, are unoccupied in (12), they constitute a pair of orthogonal fluctuations. The third orthogonal fluctuation is $\phi^\dagger = \cos(\chi_i/2)\alpha_{1i}^\dagger - \sin(\chi_i/2)\alpha_{2i}^\dagger$ which creates a pseudospin of opposite orientation. Since the classical energy is independent of the spin configuration we expect that $\phi_i^\dagger$ will not appear in the quadratic fluctuation Hamiltonian. This reflects the fact that a local spin flip does not cost energy.

For a uniform state with $\chi_i = \chi$ the Hamiltonian assumes a simple form:

$$H_{\rm fluc} = \sum_k \left\{ f_h(k) h_k^\dagger h_k + f_p(k) p_k^\dagger p_k - \frac{g(k)}{2} (p_k^\dagger h_{-k}^\dagger + p_k h_{-k}) \right\}, \tag{29}$$

where the couplings depend on χ:

$$\begin{aligned} f_h(k) &= \frac{U}{2} - \left(t_a \cos^2 \frac{\chi}{2} + t_b \sin^2 \frac{\chi}{2} \right) z\gamma_k \\ f_p(k) &= \frac{U}{2} - \left(t_a \sin^2 \frac{\chi}{2} + t_b \cos^2 \frac{\chi}{2} \right) z\gamma_k \\ g(k) &= z\gamma_k (t_a + t_b) \sin\chi . \end{aligned} \tag{30}$$

The Hamiltonian is diagonalized by a standard Bogoliubov transformation:

$$\begin{aligned} p_k &= \cosh\theta_k c_k + \sinh\theta_k d_{-k}^\dagger \\ h_k &= \cosh\theta_k d_k + \sinh\theta_k c_{-k}^\dagger \end{aligned} \tag{31}$$

which yields the excitation modes:

$$\omega_{1,2}(\boldsymbol{k}) = \tfrac{1}{2} \sqrt{U^2 - 2U(t_a + t_b) z\gamma_k + (t_a + t_b)^2 (z\gamma_k \cos\chi)^2} \pm (t_a - t_b) z\gamma_k \cos\chi . \tag{32}$$

In addition, there is a zero mode $\omega_3(\boldsymbol{k}) = 0$ corresponding to local spin flips, which reflects the macroscopic degeneracy at the classical level. Higher-order terms in the fluctuations

take into account the corrected potential landscape and generate a dispersion of the spin flip mode $\omega_3(\boldsymbol{k})$. Since here we are interested in the zero-point energy, we need not go beyond quadratic fluctuations. The quantum correction to the ground state energy is calculated from the prescription (27)

$$\Delta E(\chi) = \frac{1}{2N}\sum_k \Big[\sqrt{U^2 - 2U(t_a+t_b)z\gamma_{\boldsymbol{k}} + (t_a+t_b)^2(z\gamma_{\boldsymbol{k}}\cos\chi)^2} - U + (t_a+t_b)z\gamma_{\boldsymbol{k}}\Big] - \frac{z}{2}\left(\frac{t_a^2}{V_a} + \frac{t_b^2}{V_b}\right) \tag{33}$$

where we have added the last term perturbatively in t_α/V_α. This is justified in the regime of interest $t_\alpha, U \ll V_\alpha$. The minimum of $\Delta E(\chi)$ occurs for $\chi = \pi/2$, which corresponds to pseudospins aligned on the x–y plane. Note that the dispersions of the particle and hole excitations (32) are degenerate in this case. Their gap vanishes when $t_a + t_b = U/2z$, which marks the transition to a superfluid in agreement with the variational result (16).

To check the consistency of our fluctuation expansion the local density of fluctuations in the x–y ferromagnet can be calculated using the Bogoliubov transformation (31):

$$\langle p_i^\dagger p_i + h_i^\dagger h_i\rangle = \frac{1}{N}\sum_k 2\sinh 2\theta_k = \frac{1}{N}\sum_k\left(\frac{1 - z\gamma_{\boldsymbol{k}}(t_a+t_b)/U}{\sqrt{1 - 2z\gamma_{\boldsymbol{k}}(t_a+t_b)/U}} - 1\right). \tag{34}$$

Figure 4 plots the mean square fluctuation as a function of $(t_a + t_b)/U$ at a constant ratio t_a/t_b. It can be verified that the mean square local fluctuation is smaller than $1/4$ throughout the phase diagram. This constitutes *a posteriori* justification for our expansion which relied on the smallness of the fluctuations. We should comment though that the occupation of the zero mode cannot be calculated at this order. If the x–y state is indeed stable, interactions would generate a dispersion which would lead to a finite local ground state occupation.

We now consider Mott states with non-uniform (canted) spin order:

$$|\Psi(\theta)\rangle = \prod_{i\in A}\left(\cos\frac{\theta}{2}a_i^\dagger + \sin\frac{\theta}{2}b_i^\dagger\right)\prod_{i\in B}\left(\sin\frac{\theta}{2}a_i^\dagger + \cos\frac{\theta}{2}b_i^\dagger\right)|0\rangle. \tag{35}$$

The angle θ in this state parametrizes a continuous path from the z-Néel state ($\theta = 0$) to the x–y ferromagnet ($\theta = \pi/2$). Since $|\Psi(\theta)\rangle$ is not translationally invariant, neither will the fluctuation Hamiltonian derived from it. An elegant way to overcome this difficulty is to apply a unitary particle–hole transformation on sub-lattice B:

$$\begin{aligned} \alpha_{1i} &\leftrightarrow \alpha_{2i} \\ p_i &\leftrightarrow h_i \end{aligned} \tag{36}$$

for $i \in B$. In the spin language this is equivalent to a π rotation of the spins in the B sub-lattice about their x axis. The rotation changes the hopping terms in the Hamiltonian (1):

$$\begin{aligned} a_i^\dagger a_j + \text{h.c.} &\to a_i^\dagger a_j^\dagger + \text{h.c.} \\ b_i^\dagger b_j + \text{h.c.} &\to b_i^\dagger b_j^\dagger + \text{h.c.}, \end{aligned} \tag{37}$$

but it also transforms $|\Psi(\theta)\rangle$ to a translationally invariant state:

$$|\Psi(\theta)\rangle \to \prod_i\left(\cos\frac{\theta}{2}a_i^\dagger + \sin\frac{\theta}{2}b_i^\dagger\right)|0\rangle. \tag{38}$$

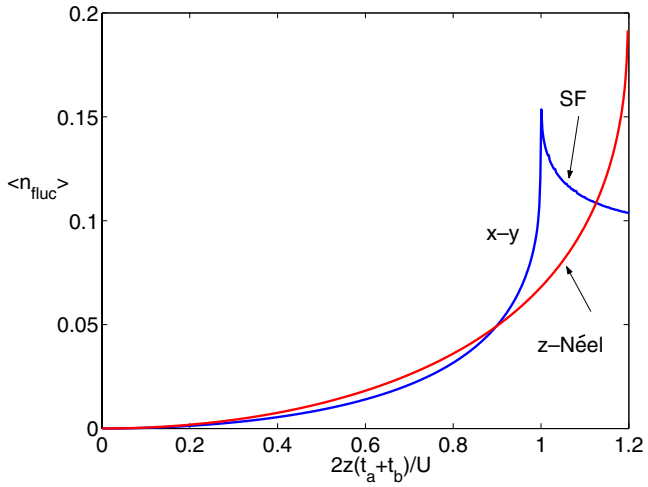

Figure 4. Mean square fluctuation in the superfluid and magnetic Mott phases. The demonstration is at a fixed ratio $t_a/t_b = 0.5$.

Our procedure can now be carried out with the new Hamiltonian and the transformed state. The fluctuation Hamiltonian assumes the form

$$\begin{aligned} H_{\text{fluc}} = \sum_k \Bigg\{ & \frac{U}{2}(p_k^\dagger p_k + h_k^\dagger h_k) - \frac{z\gamma_k}{2}\sin\theta(t_1+t_2)(p_k^\dagger h_k + \text{h.c.}) \\ & - \frac{z\gamma_k}{2}\left(t_1\cos^2\frac{\theta}{2} + t_2\sin^2\frac{\theta}{2}\right)(h_k^\dagger h_{-k}^\dagger + \text{h.c.}) \\ & - \frac{z\gamma_k}{2}\left(t_1\sin^2\frac{\theta}{2} + t_2\cos^2\frac{\theta}{2}\right)(p_k^\dagger p_{-k}^\dagger + \text{h.c.})\Bigg\} \end{aligned} \tag{39}$$

which can be diagonalized by a Bogoliubov transformation. In the z-Néel state ($\theta = 0$) the excitation energies assume a particularly simple form:

$$\omega_{1,2}(k) = \frac{U}{2}\sqrt{1 - \left(\frac{2zt_{a,b}\gamma_k}{U}\right)^2}. \tag{40}$$

Note that, contrary to the x–y state, the excitations are non-degenerate. The gap in $\omega_{1,2}(k)$ vanishes on the lines $t_{a,b} = U/2z$, respectively. Thus the z-Néel state is locally stable towards the formation of a superfluid within these boundaries. There is, however, a dangerous zero mode $\omega_3(\boldsymbol{k}) = 0$ which may be destabilized by higher-order terms in the fluctuation Hamiltonian. This mode corresponds to $\phi_k^\dagger$ which describes spin fluctuations toward the x–y ferromagnetic state. In regions where the z-Néel state is ultimately stable these corrections would just generate a dispersion for $\omega_3(\boldsymbol{k})$.

The quantum zero-point energy of the fluctuations in the z-Néel state is given by

$$\Delta E_z = \frac{U}{4}\sum_k \left[\sqrt{1 - \left(\frac{2zt_a\gamma_k}{U}\right)^2} + \sqrt{1 - \left(\frac{2zt_b\gamma_k}{U}\right)^2} - 2\right]. \tag{41}$$

The mean local fluctuation can be calculated in the same way as before:

$$\langle p_i^\dagger p_i + h_i^\dagger h_i \rangle = \frac{1}{2N} \sum_k \left[\frac{1}{\sqrt{1-(2zt_a\gamma_k/U)^2}} + \frac{1}{\sqrt{1-(2zt_b\gamma_k/U)^2}} - 2 \right]. \quad (42)$$

It is plotted in figure 4, which demonstrates that fluctuations about the z-Néel state are also small.

Before we address the full Mott domain, it is instructive to evaluate the energy corrections (33) and (41) deep in the Mott phase, where we can compare the result with the effective spin Hamiltonian (2). It is also much easier to evaluate the zero-point energy in this limit. For $t_a, t_b \ll U$ we can expand the square roots in (33) and (41) and then perform the momentum sums exactly, with the result

$$\begin{aligned} \Delta E_{xy} &\approx -\frac{z(t_a+t_b)^2}{4U} - \frac{z}{2}\left(\frac{t_a^2}{V_a} + \frac{t_b^2}{V_b}\right) \\ \Delta E_z &\approx -\frac{z(t_a^2+t_b^2)}{2U}. \end{aligned} \quad (43)$$

These are identical to the mean-field energies in the effective spin Hamiltonian (2). Thus we see that our fluctuation analysis about the variational states captures the essential spin interactions. In the next section we address the stability of the spin states over the entire parameter regime to derive a phase diagram.

A fluctuation Hamiltonian can be derived in a similar way for the superfluid phase where we find the three excitation modes:

$$\begin{aligned} \omega_{1,2}(\boldsymbol{k}) &= \frac{U}{8a}\left[t_+ \pm \sqrt{t_+ + (t_-/t_+)^2(t_+^2-1)} \right] \boldsymbol{k} + \mathrm{O}(k^2) \\ \omega_3(\boldsymbol{k}) &= U\sqrt{t_+^2 - 1 + (\boldsymbol{k}/2)^2} \end{aligned} \quad (44)$$

with $t_+ = t_a + t_b$ and $t_- = t_a - t_b$. The zero-point energy correction in the superfluid phase is evaluated using the prescription (27). A discussion of the collective modes and of the nature of the superfluid phase is deferred to the next section.

6. Phase diagram for one atom per site

In this section we combine the ingredients prepared in the last sections to present a phase diagram for a lattice with an average occupation of one atom per site. From the variational approach we found that the x–y ferromagnet becomes unstable towards a superfluid state when $t_a + t_b > U/2z$. The mean-field phase diagram was sketched in figure 3. However the boundaries of these phases with the z-Néel state remain undetermined. It is the quantum zero-point energy of fluctuations that selects ordered magnetic states from a degenerate variational energy.

To analyse the stability of the spin states we need to calculate the derivatives with respect to θ of the zero-point energies corresponding to these phases:

$$\left(\frac{\mathrm{d}^n \Delta E}{\mathrm{d}\theta^n}\right)_{\theta=\theta_0} = \sum_{\alpha,\boldsymbol{k}} \left(\frac{\mathrm{d}^n \omega_\alpha(\boldsymbol{k})}{\mathrm{d}\theta^n}\right)_{\theta=\theta_0} - \frac{\mathrm{d}^n}{\mathrm{d}\theta^n}\left((t_a^2/V_a + t_b^2/V_b) z \sin^2\frac{\theta}{2} \right)_{\theta=\theta_0}. \quad (45)$$

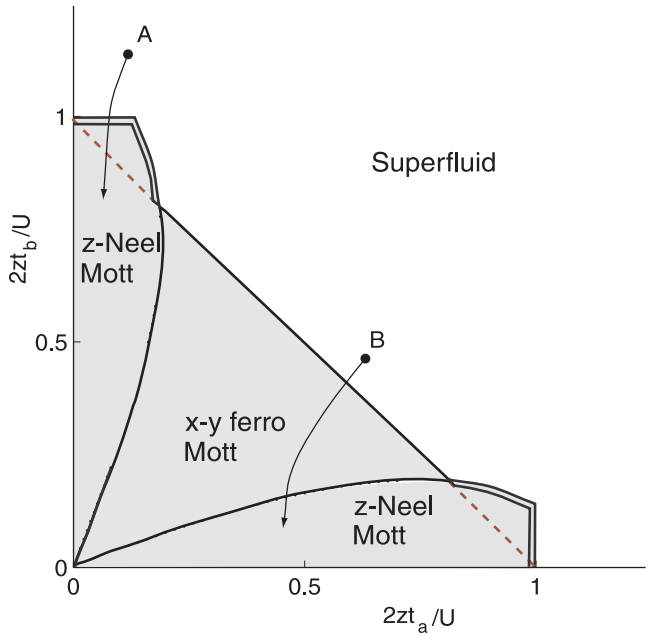

Figure 5. Phase diagram of two-component bosons at a half-filling of each species, including quantum fluctuation corrections to mean-field theory. In the filled area above the broken lines the superfluid state is metastable. Hysteretic behaviour is expected when the system is driven across the double lines.

The last term is added perturbatively in t_α/V_α and corrects for a large but finite intra-species interaction. It is easily seen that the first derivative of the modes ω_α vanishes identically at the points $\theta = 0$ and $\pi/2$, corresponding to the z-Néel and x–y states. Consequently these states are either minima or maxima of the zero-point energy. The second derivative at the z-Néel state is given by

$$\left(\frac{\mathrm{d}^2\Delta E}{\mathrm{d}\theta^2}\right)_{\theta=0} = \frac{U/2}{\tau_a - \tau_b} \times \sum_k \left(\frac{\tau_b(1-\tau_b^2\gamma_k^2)+\tau_a(1+\tau_b^2\gamma_k{}^2)}{\sqrt{1-\tau_b^2\gamma_k{}^2}} - \frac{\tau_a(1-\tau_a^2\gamma_k^2)+\tau_b(1+\tau_a^2\gamma_k{}^2)}{\sqrt{1-\tau_a^2\gamma_k{}^2}} \right) - \frac{U}{2z}\left(\frac{\tau_a^2}{v_a}+\frac{\tau_b^2}{v_b}\right) \tag{46}$$

where we have denoted $\tau_\alpha \equiv 2zt_\alpha/U$ and $v_\alpha = V_\alpha/U$. The domain of stability of the phase is obtained by numerically evaluating the momentum sum in (46). The resulting domain of stability is of the general shape illustrated in figure 5. Note that the phase boundaries deep in the Mott state ($t_{a,b} \ll U$) are linear and coincide with the result obtained from the effective Hamiltonian (2). However, we find, in contrast with the effective spin Hamiltonian, that even for true hard core interactions $V_{a,b}\to\infty$, there is a finite x–y ferromagnetic domain.

Note that the Mott z-Néel domain in figure 5 extends beyond the mean-field transition to the superfluid which occurs at $t_a + t_b = U/2z$. As seen in figure 6, this is due to a lower ground state

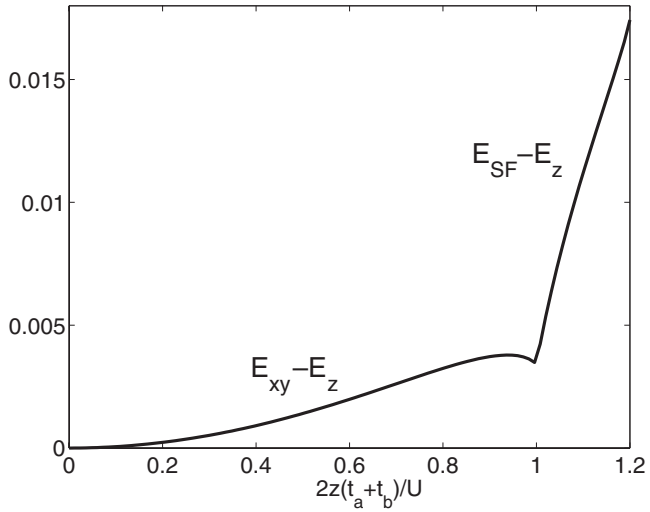

Figure 6. The energy, including quantum fluctuations, of the z-Néel state for $t_a/t_b = 0.1$.

energy (including the quantum correction) than the superfluid. In the remainder of this section we shall examine the nature of the phases and transitions in figure 5.

6.1. Metastability and hysteresis

It is an interesting observation that, over a significant parameter range, quantum fluctuations favour the z-Néel state even where its variational energy alone is higher than that of the superfluid. What kind of transition then is marked by the lines $t_{a,b} = U/2z$, where the z-Néel state finally becomes unstable? It could be one of two: (i) a first-order transition into the superfluid state or (ii) a second-order transition into a supersolid, namely a superfluid that retains Ising order.

We shall see that the former indeed occurs, but this is not immediately obvious. Consider the excitation modes (40). Since only one of them becomes gapless on the transition lines $t_{a,b} = U/2z$, one might guess that these lines mark the formation of a supersolid. However, we now show that, at the classical level, the supersolid is unstable to the formation of a uniform superfluid.

A variational state describing a supersolid is given by

$$|\Phi_{\mathrm{SS}}\rangle = \prod_{i\in A} a_i^\dagger \left(\sin\frac{\theta}{2} + \cos\frac{\theta}{2} b_i^\dagger\right) \prod_{i\in B} b_i^\dagger \left(\sin\frac{\theta}{2} + \cos\frac{\theta}{2} a_i^\dagger\right). \tag{47}$$

When $\theta = \pi$ this is just the z-Néel state. A superfluid component is added to the Néel order for $\theta < \pi$. To assess stability we parametrize, a continuous deformation of this state toward the uniform superfluid:

$$|\Phi(\delta)\rangle = \prod_i \left[\sin\frac{\theta}{2}\left(\cos\frac{\chi_i}{2} a_i^\dagger + \sin\frac{\chi_i}{2} b_i^\dagger\right) + \cos\frac{\theta}{2}\left(\sin\frac{\chi_i}{2} + \cos\frac{\chi_i}{2} a_i^\dagger b_i^\dagger\right)\right]|0\rangle \tag{48}$$

where $\chi_i = \delta, \pi/2 - \delta$ for $i \in A, B$ and $\delta \in [0, \pi/2]$. The variational energy in this state, calculated using equation (14), is

$$E(\theta, \delta) = -\frac{z(t_a + t_b)}{16} \sin 2\theta - \frac{z t_a}{16} \sin 2\theta \sin \delta. \tag{49}$$

The second derivative $(\partial E/\partial \delta)_{\delta=0}$ is negative, indicating that the supersolid is unstable. We thus establish a first-order transition between the z-Néel state and the superfluid. We should point out that, at higher order, quantum fluctuations can change the potential manifold. In particular, they can make the supersolid phase locally stable. This interesting possibility can be checked, for example, by quantum Monte Carlo simulations. However, at our level of approximation there is a first-order transition directly to the uniform superfluid.

An important implication is the presence of a hysteresis region. Consider a change of system parameters from the superfluid to the z-Néel state along route A in figure 5. In the region where the superfluid is metastable, it may take an excessively long time to nucleate the z-Néel state. The system is thus likely to remain in the superfluid state until its line of metastability is crossed (broken lines in figure 5). Passing the same route in the opposite direction the z-Néel state will, of course, persist up to the transition line. Along route B matters are qualitatively different. Since the transition into the x–y Mott state is continuous, there is no hysteresis there. The transition from the x–y to the z-Néel state is first order but without a significant hysteresis region. In fact, it is well described as a transition from easy-axis to easy-plane anisotropy in the Heisenberg model (2).

6.2. The superfluid and the x–y ferromagnet

The uniform superfluid phase deserves a closer examination. In several aspects, it is different from the single-component case. Most importantly, the two-component superfluid is intimately related to the x–y ferromagnet.

In terms of the bosonic operators, the x–y ferromagnetic Mott state sustains an order parameter $\langle a^\dagger b \rangle \neq 0$. In this sense it can be viewed as a counterflow superfluid [7]. It can support supercurrents of relative motion characterized by a gradient of the relative phase between a and b atoms. In the spin language this is simply a gradient of the spin orientation on the x–y plane. A magnetic field gradient, $h(\boldsymbol{x}) = h_0 x$ in (2), would twist the spin configuration at a constant rate inducing AC super-counterflow of frequency $\omega = h_0 L$. The Goldstone mode associated with this order is a spin wave, which describes fluctuations of the relative phase between the two components. We should note again that, in the quadratic fluctuation Hamiltonian (25), spin waves are dispersionless. This is a direct consequence of the spin degeneracy at the classical (variational) level. However, it does not indicate truly vanishing spin wave stiffness. Indeed, higher-order terms in the fluctuations generate a finite linear spin wave dispersion. This can also be understood from the effective spin Hamiltonian (2), which obviously has a finite spin stiffness $\propto J_\perp$.

As system parameters are varied across the transition at $t_a + t_b = U/2z$, one of the gapped particle–hole fluctuations of the x–y Mott state condenses, marking the formation of the two superfluid order parameters $\langle a \rangle$ and $\langle b \rangle$. As pointed out in [19], in the x–y Mott state only the relative phase is fixed while the average phase of the two components is disordered. In the superfluid the average phase orders as well. Accordingly we find two linear gapless modes in the superfluid (44), corresponding to an in-phase fluctuation of the two components $(\omega_1(\boldsymbol{k}))$, and a relative phase, spin wave fluctuation $\omega_2(\boldsymbol{k})$. From these considerations it is obvious that the universal aspects of the transition will be identical to the standard, single-component Mott transition [19].

7. Discussion and conclusions

We have shown that the magnetic phases found earlier by the perturbative treatments [7, 8] persist up to the superfluid transition. In fact, they modify this transition in an interesting way, adding lines of *first-order* transition between a uniform superfluid and a z-Néel (checkerboard) Mott state. It is interesting to consider the present results in light of the current experimental possibilities. In particular the high energy scales, comparable to the on-site repulsion, associated with spin ordering close to the Mott–superfluid transition, facilitate experimental observations of these phases. For the same reason they are also expected to be robust to perturbations due to, for example, inhomogeneous magnetic field variations. The existence of first-order transitions and metastable states in this regime indicates that the system is likely to display interesting dynamics as the optical potential is lowered across the transition point. In particular it is expected to display hysteretic behaviour and nucleation kinetics. It would be interesting to study the effects of a global confining potential on the phases we described. For instance, we showed that spin ordered Mott states with equal filling of the two species are qualitatively different for odd and even numbers of particles per site. Both are likely to be observable in any realistic realization, since the inhomogeneous trapping potential typically leads to domains with different occupations.

Finally, it is important to note that detection of the complex states, of the type discussed in this paper, presents an interesting challenge in its own right. It turns out that the quantum nature of strongly correlated magnetic states can be revealed by *spatial noise* correlations in the image of the expanding gas [20]. Specifically, atoms released from a Mott-insulating state of the optical lattice display sharp (Bragg) peaks in the density–density correlation function as a consequence of quantum statistics. Such peaks can be used to probe the spin-ordered Mott states proposed for two-component bosons.

In summary, we presented a theoretical analysis of the phase diagram of two-component bosons on an optical lattice. We extended earlier treatments which were valid only deep in the Mott phase toward the MI–SF transition and beyond and were thus able to map a complete phase diagram.

Acknowledgments

We would like to thank L Mathey, L Duan, A Imembakov, I Bloch, A Sorensen and D W Wang for useful discussions. This work was supported by ARO, NSF (PHY-0134776, DMR-0132874), Sloan Foundation, Packard Foundation and the German Science Foundation (DFG).

References

[1] Greiner M *et al* 2002 *Nature* **415** 39
[2] Orzel C *et al* 2001 *Science* **291** 2386
[3] Jaksch D *et al* 1998 *Phys. Rev. Lett.* **81** 3108
[4] Demler E and Zhou F 2002 *Phys. Rev. Lett.* **88** 163001
[5] Hofstetter W *et al* 2002 *Phys. Rev. Lett.* **89** 220407
[6] Recati A *et al* 2003 *Phys. Rev. Lett.* **90** 049901
Paredes B and Cirac J I 2003 *Phys. Rev. Lett.* **90** 150402
[7] Kuklov A B and Svistunov B V 2003 *Phys. Rev. Lett.* **90** 100401
[8] Duan L-M, Demler E and Lukin M D 2003 *Phys. Rev. Lett.* **91** 090402

[9] Lloyd S 1996 *Science* **273** 1073
Sorensen A and Molmer K 1999 *Phys. Rev. Lett.* **83** 2274
[10] Gross K *et al* 2002 *Phys. Rev.* A **66** 033603
[11] Mandel O *et al* 2003 *Phys. Rev. Lett.* **91** 010407
[12] Fisher M P A *et al* 1989 *Phys. Rev.* B **40** 546
[13] Imembakov A, Lukin M D and Demler E 2003 *Preprint* cond-mat/0306204
[14] Snoek M and Zhou F 2003 *Preprint* cond-mat/0306198
[15] Sheshadri K, Krishnamurthy H R, Pandit R and Ramakrishnan T V 1993 *Europhys. Lett.* **22** 257
[16] Rokhsar D S and Kotliar B G 1991 *Phys. Rev.* B **44** 10328
[17] Moessner R 2001 *Can. J. Phys.* **79** 1283
[18] Shender E F 1982 *Sov. Phys.—JETP* **56** 178
[19] Kuklov A, Prokof'ev N and Svistunov B 2003 *Preprint* cond-mat/0305694
[20] Altman E *et al* 2003 *Preprint* cond-mat/0306226